Chemical Science

EDGE ARTICLE

View Article Online
View Journal | View Issue

Cite this: *Chem. Sci.*, 2017, **8**, 3832

Shape-transformable liquid metal nanoparticles in aqueous solution†

Yiliang Lin,[a] Yang Liu,[b] Jan Genzer*[a] and Michael D. Dickey*[a]

Received 5th January 2017
Accepted 22nd February 2017

DOI: 10.1039/c7sc00057j

rsc.li/chemical-science

Stable suspensions of eutectic gallium indium (EGaIn) liquid metal nanoparticles form by probe-sonicating the metal in an aqueous solution. Positively-charged molecular or macromolecular surfactants in the solution, such as cetrimonium bromide or lysozyme, respectively, stabilize the suspension by interacting with the negative charges of the surface oxide that forms on the metal. The liquid metal breaks up into nanospheres *via* sonication, yet can transform into rods of gallium oxide monohydroxide (GaOOH) *via* moderate heating in solution either during or after sonication. Whereas heating typically drives phase transitions from solid to liquid (*via* melting), here heating drives the transformation of particles from liquid to solid *via* oxidation. Interestingly, indium nanoparticles form during the process of shape transformation due to the selective removal of gallium. This dealloying provides a mechanism to create indium nanoparticles at temperatures well below the melting point of indium. To demonstrate the versatility, we show that it is possible to shape transform and dealloy other alloys of gallium including ternary liquid metal alloys. Scanning transmission electron microscopy (STEM), energy-dispersive X-ray spectroscopy (EDS) mapping, and X-ray diffraction (XRD) confirm the dealloying and transformation mechanism.

Introduction

Metals that are liquid at room temperature are notable for having fluidity and metallic conductivity. Mercury is a familiar liquid metal with limited applications due to its toxicity.[1] Gallium (melting point, mp 29.8 °C) and its alloys, such as eutectic gallium indium (EGaIn,[2] mp 15.5 °C) and gallium indium tin (Galinstan,[3] mp −19 °C), are promising alternatives to mercury due to their negligible vapor pressure[4] and low-toxicity.[5] Gallium-based liquid metals have applications in microfluidic systems and soft electronics,[6] such as stretchable wires,[7] soft circuits,[8] inductors,[9] antennas,[10] pumps,[11] electrodes,[12] sensors[13] and memristors.[14] In particular, colloidal droplets of liquid metal have applications as pumps,[11] mixers,[15] sensors,[16] soft circuit elements,[17] catalysts,[18] and drug delivery systems.[5]

While liquid metal particles can be obtained by molding[19] or microfluidics,[20] sonication offers a simple way to manufacture liquid metal particles. It is possible to form nanoparticles by sonicating liquid metal in ethanol[21] or 2-propanol.[22] However, simply sonicating liquid metal in water leads to an unstable suspension.[11] The synthesis of stable liquid metal nanoparticles in aqueous solution would benefit applications that utilize water, such as drug delivery, microfluidics, and electrochemistry.

Here, we report on the formation of a stable suspension of liquid metal nanoparticles in an aqueous solution of positively-charged surfactants, formed within 10 minutes, by sonication. The resulting spherical nanoparticles transform into rods of gallium oxide monohydroxide (GaOOH) *via* an oxidation reaction which is driven by exposing the nanoparticles to elevated temperatures in water during or after sonication. The ability to transform the shape of a particle is exciting because shape plays an important role in both the individual and cooperative behavior of colloids and colloidal assemblies. For example, shape transforming particles have potential applications for drug delivery,[23] catalysis,[24] colloidal jamming[25] and optics.[26]

The ability to selectively strip gallium from gallium alloys also offers a simple route for dealloying. Dealloying can purify materials and create morphologies that would be difficult to form otherwise.[27] The separation of indium and gallium involves typically high-temperature processing, use of chemical agents (*e.g.* alkaline or acidic medium), or electrolysis[28], and a recent paper[29] reports using $NaBH_4$ to selectively remove gallium from Galinstan. In contrast, the method here only requires mild heating in an aqueous solution to effectively enrich the particles with indium. Consequently, dealloying provides a way to produce indium nanoparticles significantly below the temperatures used with existing methods to produce these particles.[30]

[a]*Department of Chemical & Biomolecular Engineering, North Carolina State University, Raleigh, NC 27695-7905, USA. E-mail: jgenzer@ncsu.edu; mddickey@ncsu.edu*

[b]*Department of Materials Science & Engineering, North Carolina State University, Raleigh, NC 27695-7907, USA*

† Electronic supplementary information (ESI) available. See DOI: 10.1039/c7sc00057j

Here, we describe these shape-changing liquid metal particles and the accompanying dealloying process that occurs by selective oxidation of gallium in a binary or ternary liquid metal alloy.

Results and discussion

To produce liquid metal nanoparticles, 0.2 g of liquid metal (EGaIn, gallium, or Galinstan) was added into a 20 ml vial filled with 10 ml of deionized (DI) water and 2 mg of lysozyme (Lys, Sigma-Aldrich). Lys is an inexpensive, positively-charged protein (the isoelectric point is ~11.4) found in chicken egg whites. We chose Lys due to its affinity to oxide surfaces. Probe sonication produced a grey suspension within 10 min. The suspension without Lys precipitated within 1 hour, while those suspensions (both gallium and EGaIn) with Lys remained stable, as shown in Fig. S1.† Transmission electron microscopy (TEM) images confirmed the presence of sub-micron sized rods, as shown in Fig. 1a, which was unexpected considering that spherical structures normally form in ethanol following an identical sonication process.[8] Micrographs of the samples taken at time increments during the sonication process showed that rods formed after 5 min of sonication, as shown in Fig. S2.† Sonication produced some foam above the liquid. Samples taken from the foam also contained rods (Fig. S3†). The Lys solutions that were sonicated without liquid metal did not produce foam, suggesting that the rods help to stabilize the foam. Particles are known to help stabilize foams and in particular, anisotropic rod-shaped particles stabilize foams[31] significantly better than spherical ones.[32]

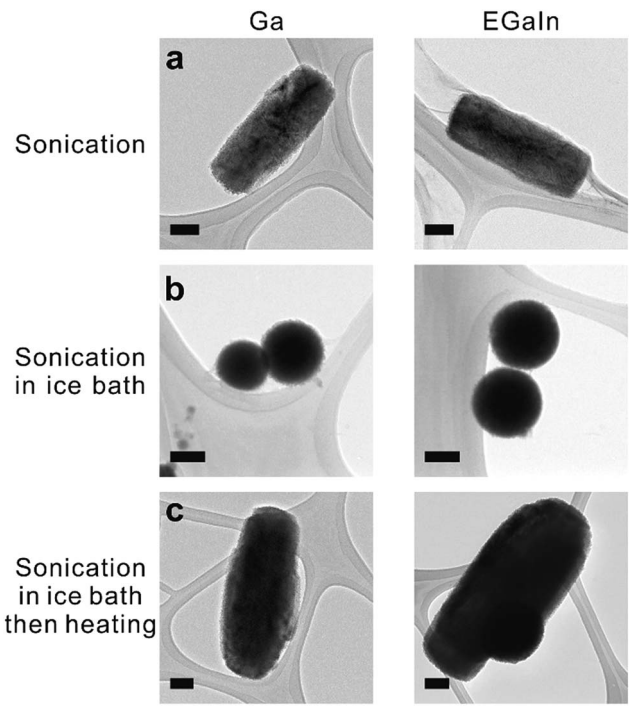

Fig. 1 TEM images of liquid metal nanoparticles. (a) Rods obtained from sonicating gallium (left column) and EGaIn (right column) in aqueous solution in the presence of Lys protein. (b) Nanospheres synthesized by repeating (a) while using an ice bath. (c) Rods obtained from post heating the spheres from (b). The scale bars are 100 nm.

We noticed that the vial became hot (in some cases as warm as 80 °C) during sonication of the solution. Thus, we repeated the same sonication experiments in an ice bath, which resulted in the formation of nanospheres, as shown in Fig. 1b (multiple-particle image with the size distribution shown in Fig. S4†). These spherical nanoparticles transform into rods after heating the solution to 70 °C for half an hour (Fig. 1c), which proves that heat, rather than sonication, transforms their shape.

To comprehend this phenomenon, we first characterized the samples that were obtained by sonication (Fig. 1a) using X-ray diffraction (XRD). Fig. 2a reveals that the samples contain both metallic indium and crystalline gallium oxide hydroxide (GaOOH). GaOOH crystals are known to be rod-like,[33] which is consistent with the shape observed here. Selected-area electron diffraction (SAED) (Fig. 2b(2)) confirms that the rods correspond to the GaOOH crystalline phase. While the diffraction indicates a single crystal, defects in the crystal were observed in the diffraction pattern after prolonged high-resolution TEM imaging, indicating damage from the intensive electron beam (Fig. S5†). A high-resolution TEM (HRTEM) image (Fig. 2b(3)) and its Fast Fourier Transform (FFT) image (Fig. 2b(4)) also confirm that the lattice structure became highly defective after electron beam exposure. Energy-dispersive X-ray spectroscopy (EDS) mapping on an FEI Titan scanning transmission electron microscope (STEM) with ChemiSTEM Technology (Fig. 2c) shows clearly that the rod structures lack indium while the spherical nanoparticles contain only indium. This morphology is consistent with the fact that gallium is much more reactive than indium and prefers to form GaOOH in water.[34] Thus, during heating, gallium oxidizes to form GaOOH crystals and the remaining alloy becomes enriched with indium due to the consumption of gallium. This phenomenon can be explained by the shift in the alloy phase diagram[35] and is somewhat analogous to the phase separation that occurs by cooling liquid metal particles.[36]

Fig. 2d depicts the steps of the morphological transformation captured by STEM. After sonication in an ice bath (stage 1), the liquid metal breaks into nanoparticles composed of gallium and indium. Quantification of the amount of gallium and indium at site 1 shows that the particle is composed of 70.75 ± 6.60 wt% gallium (3σ) and 29.25 ± 4.87 wt% indium (3σ), which is the same as the chemical composition of the bulk alloy within experimental uncertainty. This finding shows that sonication of liquid metal in the presence of Lys enables the formation of stable suspensions of liquid metal nanospheres in aqueous solution. In contrast, it would be difficult to form particles of gallium-alloys *via* bottom-up approaches due to the difficulty of reducing gallium salt precursors. After heating the nanospherical particles at 70 °C for ~20 min (stage 2), some GaOOH rods begin to appear on the surface of the liquid metal particles. The particles at site 2 and site 3 consist of only 32.09 wt% and 14.25 wt% gallium, respectively, which proves that during the formation of the GaOOH crystals the gallium in the alloy particles gets consumed. The nanoparticles therefore become enriched with indium relative to the bulk metal.

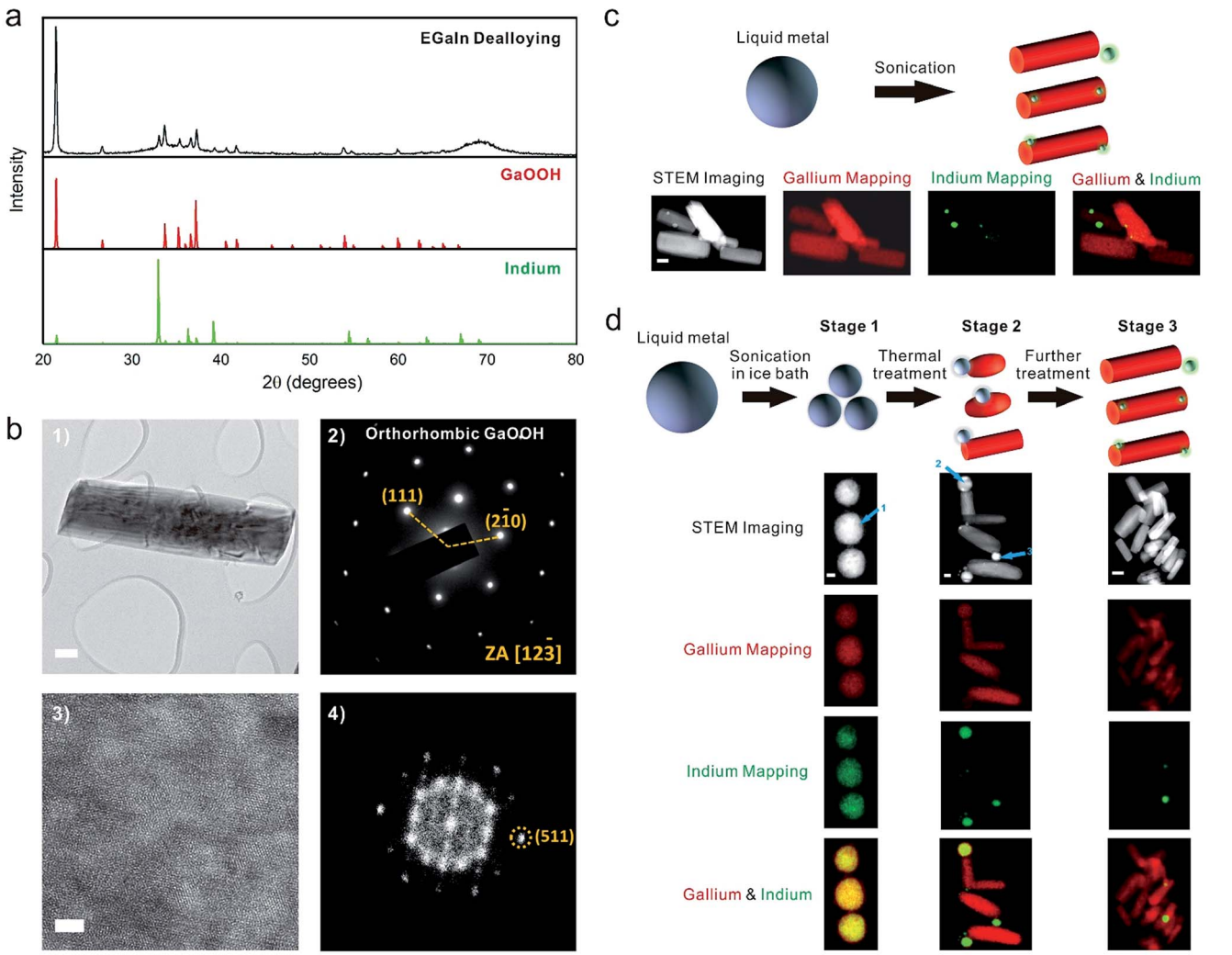

Fig. 2 Characterization of the liquid metal (EGaIn) nanomaterials along with a proposed mechanism for the shape transformation and dealloying. (a) XRD spectra of the particles taken after sonication and the spectra for standard GaOOH (PDF 04-010-9861) and indium (PDF 01-080-5356). (b) (1) TEM image of the GaOOH rods; (2) selected-area electron diffraction (SAED) pattern from the red region in image (1), which can be indexed to an orthorhombic GaOOH phase; (3) and (4) high-resolution TEM (HRTEM) image and its Fast Fourier Transform (FFT) image, showing the defective lattice structure from prolonged exposure to the intensive electron beam. The scale bars are 100 and 3 nm. (c) Synthesis of GaOOH from direct sonication and the corresponding STEM image and EDS mapping. The scale bar is 100 nm. (d) Mechanism for the shape transformation and the corresponding STEM image and EDS mapping. The scale bars are 30, 100, and 300 nm for stage 1, stage 2, and stage 3, respectively.

Micrographs of the samples at this stage show that most of the GaOOH rods are attached to a single particle enriched with indium. The total mass ratio of gallium/indium within the region (containing multiple rods and nanospheres) is the same as the starting liquid metal alloy (3 : 1) within the error margin, which suggests that a rod attached to a particle originates from the same initial spherical particle. With additional heating, the liquid metal particles transform completely to GaOOH rods and indium particles (stage 3). We found that some of the indium particles break away from the GaOOH rod structures (perhaps during TEM sample preparation). Consequently, the total mass ratio of gallium/indium in this region deviates from the expected 3 : 1 ratio.

The ability to form GaOOH in a simple manner is appealing. GaOOH is an important precursor in the semiconductor industry and a number of methods exist for its formation. GaOOH rods (also called spindles) are known to form *via* hydrothermal methods using gallium salts.[37] It is also possible to use laser ablation on molten gallium to generate GaOOH in the presence of surfactants.[38] However, most of these methods involve extensive aging (tens of hours to several days). In addition, it is possible to form GaOOH by ultrasonicating gallium in water,[39] however, it normally takes up to 2 hours to convert it fully into GaOOH. The method described here offers a route to rapidly convert liquid metal spheres into GaOOH. In our studies, the rod structures appear to consist of stacked flakes, which is consistent with previous observations.[33] Earlier research attributed this rod formation to sonochemistry.[33,40] The results here show that sonication only helps to break the liquid metal into sized spheres. The formation of the rods is

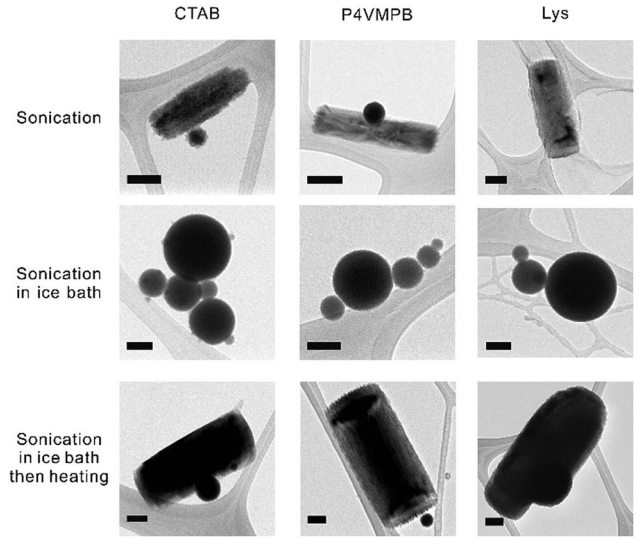

Fig. 3 TEM micrographs depicting liquid metal nanomaterials stabilized with different positively-charged surfactants, including small molecule cetrimonium bromide (CTAB), synthetic polymer poly(4-vinyl-1-methyl-pyridinium bromide) (P4VMPB), and protein lysozyme (Lys). The particle morphology was the same for all three positively-charged surfactants. The scale bars are 100 nm.

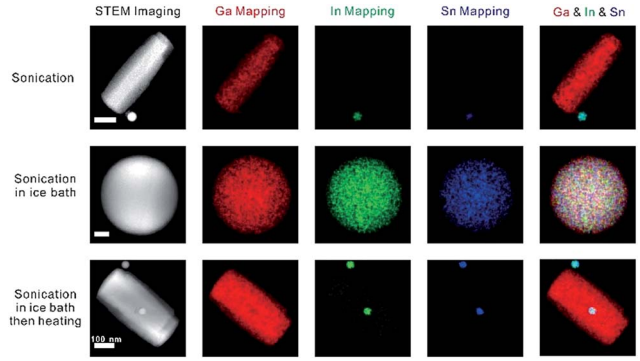

Fig. 4 Characterization of the liquid metal (Galinstan) materials using STEM-EDS. EDS mapping of the rods and nanosphere obtained from sonication. The scale bars are (from top to bottom) 100, 20, and 100 nm.

driven thermally. In addition to forming rods of GaOOH, the method also provides a pathway to synthesize indium particles below the melting point of indium.

Our experiments indicate that surfactants play an important role in the synthesis and shape transformation process and we further investigated different positively-charged surfactants, including cetrimonium bromide (CTAB), poly(4-vinyl-1-methyl-pyridinium bromide) (P4VMPB), and lysozyme (Lys). Fig. 3 shows that regardless of the size of the positively-charged surfactant, the presence of positive charges on the surfactant molecules causes the liquid metal to form rods within 10 min of sonication (or be transformed into rods from liquid metal particles by thermal treatment). Other positively-charged surfactants, such as cytochrome C from equine heart and polyethyleneimine, behave similarly to Lys (Fig. S6†). Within the same sonication time, well-defined rod structures do not form in aqueous solution without a surfactant nor with negatively-charged surfactants, regardless of the size of the surfactant (Fig. S7†). We confirmed that the rods synthesized with CTAB, P4VMPB and Lys have positive zeta potentials (+10.8, +22.5, and +15.1 mV respectively). We performed XPS experiments to prove that Lys binds strongly to the native oxide on liquid metal, but does not appear to react covalently with it (Fig. S8†). These measurements suggest that the surfactant interacts electrostatically with the particle surface. These benchmark experiments show that (1) positively-charged surfactants interact with metal/metal oxide surfaces, which are typically negatively-charged; (2) positively-charged surfactants help to stabilize the rods to prevent aggregation.

We added glutaraldehyde (GA) to crosslink the Lys to further understand the shape transformation phenomenon. In one experiment, we added GA prior to sonication and in another, we added GA after sonication but before heating. In both cases, the nanoparticles maintained a spherical shape throughout the whole process. The crosslinked Lys on the surface of the spheres could confine the geometry, preventing it from forming rods and/or hinder reactions between water and gallium (Fig. S9†). Either way, this result further proves that Lys is present on the surface of the particles.

In order to demonstrate that the synthesis strategy and dealloying phenomenon is not limited to a binary liquid metal alloy system, we sonicated Galinstan in aqueous solution in the presence of Lys. As expected, sonication in an ice bath produced stable Galinstan spherical nanoparticles, whereas GaOOH rods formed during the post-heating stage, as shown in Fig. 4. While the rods contain gallium, the particles contain both indium and tin, which further proves the hypothesis that during the sonication gallium reacts with water to form GaOOH, enriching the indium and tin elements in the spherical nanoparticles.

The approaches described herein are not without drawbacks. Sonication in an ice bath without further processing produces particles with polydisperse sizes and the aspect ratio of the rods also varies. Future work could optimize the synthesis of uniform particles by applying pulse sonication or gradient centrifugation. Depending on the application, separation of indium or indium/tin nanoparticles from the GaOOH rods may also be necessary; alternatively pure gallium can be used to produce GaOOH without the formation of metal nanoparticles *via* dealloying.

Conclusions

In summary, this paper reports a facile way to produce stable liquid metal spherical particles in aqueous solution in the presence of positively-charged surfactants. The spherical particles transform into GaOOH rods simply through thermal control of the solution due to the reactivity of gallium. Crosslinking the surfactant on the spherical particles prevents the particles from transforming into rods during heat treatment. In benchmark experiments with negatively-charged surfactants or without any surfactants, the rods did not form within the same reaction time. One interesting outcome of this work is that heating causes particles to not only change shape, but also change phase from

liquid to solid; normally heating causes the opposite transition *via* melting. These shape-changing and phase-transforming particles have potential applications in drug delivery, catalysis, colloidal jamming, and optics. Finally, during the process of shape-transformation, the liquid metal dealloys, which also offers a simple route for separating indium and forming indium nanoparticles at low temperatures. The synthesis and dealloying strategy also works with ternary liquid metal alloys.

Methods

Liquid metal suspension preparation and characterization

To form a suspension of liquid metal (gallium, EGaIn, Galinstan), 0.2 g of liquid metal was added into a vial (20 ml), which was filled with DI water to a total volume of 10 ml and 2 mg of surfactant. A Q55 Sonicator (QSONICA) was used for sonication (frequency: 20 kHz; power rating: 55 watts; standard probe 1/8″). The amplitude of the sonicator was adjusted to 80 and the sonication proceeded for 10 min. The post-heating treatment was achieved by heating the solution at 70 °C for 30 min without stirring. For scanning electron microscope (SEM) characterization, the suspension was diluted 50 times and deposited drop-wise onto a clean silicon wafer. After drying in air, the sample was examined by SEM (FEI Verios 460L) operated at 2 kV. For TEM/STEM characterization, the suspension was diluted 50 times and cast onto a TEM lacey carbon grid (300 mesh) (Ted Pella). After drying in air, the sample was probed by TEM/STEM (JEOL 2010F and FEI Titan 80-300), operated at 200 kV. For XRD characterization, the suspension was deposited onto a clean silicon wafer. After drying in air, the sample was processed by a Rigaku SmartLab X-ray Diffractometer.

Author contribution

Y. L., J. G. and M. D. designed the project. Y. L. and Y. L. performed the experiments. Y. L., J. G. and M. D. wrote the paper. All authors analysed and interpreted the data.

Acknowledgements

The authors acknowledge funding from the National Science Foundation and the Research Triangle MRSEC (DMR-1121107). We thank Mr Carlos Cruz and Dr Balaji Rao for providing protein samples. The authors thank Yue Lu for helpful discussions. The authors acknowledge the use of the Analytical Instrumentation Facility (AIF) at North Carolina State University, which is supported by the State of North Carolina and the National Science Foundation (award number ECCS-1542015). The AIF is a member of the North Carolina Research Triangle Nanotechnology Network (RTNN), a site in the National Nanotechnology Coordinated Infrastructure (NNCI).

References

1 T. W. Clarkson and L. Magos, *Crit. Rev. Toxicol.*, 2006, **36**, 609–662.
2 M. D. Dickey, R. C. Chiechi, R. J. Larsen, E. A. Weiss, D. A. Weitz and G. M. Whitesides, *Adv. Funct. Mater.*, 2008, **18**, 1097–1104.
3 T. Liu, P. Sen and C. J. Kim, *J. Microelectromech. Syst.*, 2012, **21**, 443–450.
4 F. Geiger, C. A. Busse and R. I. Loehrke, *Int. J. Thermophys.*, 1987, **8**, 425–436.
5 (*a*) W. M. Haynes, *CRC Handbook of Chemistry and Physics*, CRC Press, 95th edn, 2014; (*b*) Y. Lu, Q. Hu, Y. Lin, D. B. Pacardo, C. Wang, W. Sun, F. S. Ligler, M. D. Dickey and Z. Gu, *Nat. Commun.*, 2015, **6**, 10066.
6 (*a*) M. D. Dickey, *ACS Appl. Mater. Interfaces*, 2014, **6**, 18369–18379; (*b*) K. Khoshmanesh, S. Tang, J. Y. Zhu, S. Schaefer, A. Mitchell, K. Kalantar-zadeh and M. Dickey, *Lab Chip*, 2017, DOI: 10.1039/c7lc00046d.
7 (*a*) E. Palleau, S. Reece, S. C. Desai, M. E. Smith and M. D. Dickey, *Adv. Mater.*, 2013, **25**, 1589–1592; (*b*) S. Zhu, J.-H. So, R. Mays, S. Desai, W. R. Barnes, B. Pourdeyhimi and M. D. Dickey, *Adv. Funct. Mater.*, 2013, **23**, 2308–2314; (*c*) K. P. Mineart, Y. Lin, S. C. Desai, A. S. Krishnan, R. J. Spontak and M. D. Dickey, *Soft Matter*, 2013, **9**, 7695.
8 Y. Lin, C. Cooper, M. Wang, J. J. Adams, J. Genzer and M. D. Dickey, *Small*, 2015, **11**, 6397–6403.
9 (*a*) N. Lazarus, C. D. Meyer and W. J. Turner, *RSC Adv.*, 2015, **5**, 78695–78700; (*b*) N. Lazarus, C. D. Meyer, S. S. Bedair, H. Nochetto and I. M. Kierzewski, *Smart Mater. Struct.*, 2014, **23**, 85036.
10 (*a*) S. Cheng, A. Rydberg, K. Hjort and Z. Wu, *Appl. Phys. Lett.*, 2009, **94**, 144103; (*b*) G. J. Hayes, J. H. So, A. Qusba, M. D. Dickey and G. Lazzi, *IEEE Trans. Antennas Propag.*, 2012, **60**, 2151–2156; (*c*) Y. Huang, Y. Wang, L. Xiao, H. Liu, W. Dong and Z. Yin, *Lab Chip*, 2014, **14**, 4205–4212; (*d*) M. R. Khan, G. J. Hayes, J.-H. So, G. Lazzi and M. D. Dickey, *Appl. Phys. Lett.*, 2011, **99**, 13501; (*e*) M. Kubo, X. Li, C. Kim, M. Hashimoto, B. J. Wiley, D. Ham and G. M. Whitesides, *Adv. Mater.*, 2010, **22**, 2749–2752; (*f*) A. M. Morishita, C. K. Y. Kitamura, A. T. Ohta and W. A. Shiroma, *IEEE Antenn. Wireless Propag. Lett.*, 2013, **12**, 1388–1391; (*g*) J.-H. So, J. Thelen, A. Qusba, G. J. Hayes, G. Lazzi and M. D. Dickey, *Adv. Funct. Mater.*, 2009, **19**, 3632–3637; (*h*) M. Jobs, K. Hjort, A. Rydberg and Z. Wu, *Small*, 2013, **9**, 3230–3234.
11 (*a*) S.-Y. Tang, K. Khoshmanesh, V. Sivan, P. Petersen, A. P. O'Mullane, D. Abbott, A. Mitchell and K. Kalantar-zadeh, *Proc. Natl. Acad. Sci. U. S. A.*, 2014, **111**, 3304–3309; (*b*) M. Gao and L. Gui, *Lab Chip*, 2014, **14**, 1866–1872.
12 (*a*) J.-H. So and M. D. Dickey, *Lab Chip*, 2011, **11**, 905; (*b*) N. Hallfors, A. Khan, M. D. Dickey and A. M. Taylor, *Lab Chip*, 2013, **13**, 522–526; (*c*) A. L. Richards, M. D. Dickey, A. S. Kennedy and G. D. Buckner, *J. Micromech. Microeng.*, 2012, **22**, 115012.
13 (*a*) D. J. Lipomi, M. Vosgueritchian, B. C.-K. Tee, S. L. Hellstrom, J. A. Lee, C. H. Fox and Z. Bao, *Nat. Nanotechnol.*, 2011, **6**, 788–792; (*b*) C. Majidi, R. Kramer and R. J. Wood, *Smart Mater. Struct.*, 2011, **20**, 105017; (*c*) Y. Mengüç, Y.-L. Park, H. Pei, D. Vogt, P. M. Aubin, E. Winchell, L. Fluke, L. Stirling, R. J. Wood and

C. J. Walsh, *Int. J. Robot. Res.*, 2014, 278364914543793; (*d*) Y.-L. Park, C. Majidi, R. Kramer, P. Bérard and R. J. Wood, *J. Micromech. Microeng.*, 2010, **20**, 125029; (*e*) R. D. Ponce Wong, J. D. Posner and V. J. Santos, *Sens. Actuators, A*, 2012, **179**, 62–69; (*f*) R. K. Kramer, C. Majidi, R. Sahai and R. J. Wood, in *2011 IEEE/RSJ International Conference on Intelligent Robots and Systems (IROS)*, 2011, pp. 1919–1926.

14 H.-J. Koo, J.-H. So, M. D. Dickey and O. D. Velev, *Adv. Mater.*, 2011, **23**, 3559–3564.

15 S.-Y. Tang, V. Sivan, P. Petersen, W. Zhang, P. D. Morrison, K. Kalantar-zadeh, A. Mitchell and K. Khoshmanesh, *Adv. Funct. Mater.*, 2014, **24**, 5851–5858.

16 S.-Y. Tang, B. Ayan, N. Nama, Y. Bian, J. P. Lata, X. Guo and T. J. Huang, *Small*, 2016, **12**, 3861–3869.

17 J. W. Boley, E. L. White and R. K. Kramer, *Adv. Mater.*, 2015, **27**, 2355–2360.

18 F. Hoshyargar, J. Crawford and A. P. O'Mullane, *J. Am. Chem. Soc.*, 2017, **139**, 1464–1471.

19 M. Mohammed, A. Xenakis and M. Dickey, *Metals*, 2014, **4**, 465–476.

20 (*a*) J. Thelen, M. D. Dickey and T. Ward, *Lab Chip*, 2012, **12**, 3961; (*b*) S.-Y. Tang, I. D. Joshipura, Y. Lin, K. Kalantar-Zadeh, A. Mitchell, K. Khoshmanesh and M. D. Dickey, *Adv. Mater.*, 2016, **28**, 604–609; (*c*) T. Hutter, W.-A. C. Bauer, S. R. Elliott and W. T. S. Huck, *Adv. Funct. Mater.*, 2012, **22**, 2624–2631.

21 J. N. Hohman, M. Kim, G. A. Wadsworth, H. R. Bednar, J. Jiang, M. A. LeThai and P. S. Weiss, *Nano Lett.*, 2011, **11**, 5104–5110.

22 A. Yamaguchi, Y. Mashima and T. Iyoda, *Angew. Chem., Int. Ed.*, 2015, **54**, 12809–12813.

23 (*a*) S. Venkataraman, J. L. Hedrick, Z. Y. Ong, C. Yang, P. L. R. Ee, P. T. Hammond and Y. Y. Yang, *Adv. Drug Delivery Rev.*, 2011, **63**, 1228–1246; (*b*) J. A. Champion, Y. K. Katare and S. Mitragotri, *J. Controlled Release*, 2007, **121**, 3–9.

24 (*a*) R. Narayanan and M. A. El-Sayed, *J. Phys. Chem. B*, 2005, **109**, 12663–12676; (*b*) A. R. Tao, S. Habas and P. Yang, *Small*, 2008, **4**, 310–325.

25 (*a*) A. Donev, I. Cisse, D. Sachs, E. A. Variano, F. H. Stillinger, R. Connelly, S. Torquato and P. M. Chaikin, *Science*, 2004, **303**, 990–993; (*b*) A. Donev, R. Connelly, F. H. Stillinger and S. Torquato, *Phys. Rev. E: Stat., Nonlinear, Soft Matter Phys.*, 2007, **75**, 51304.

26 (*a*) C. M. Cobley, S. E. Skrabalak, D. J. Campbell and Y. Xia, *Plasmonics*, 2009, **4**, 171–179; (*b*) C. J. Murphy, T. K. Sau, A. M. Gole, C. J. Orendorff, J. Gao, L. Gou, S. E. Hunyadi and T. Li, *J. Phys. Chem. B*, 2005, **109**, 13857–13870.

27 (*a*) X. Lu, L. Au, J. McLellan, Z.-Y. Li, M. Marquez and Y. Xia, *Nano Lett.*, 2007, **7**, 1764–1769; (*b*) J. Erlebacher, M. J. Aziz, A. Karma, N. Dimitrov and K. Sieradzki, *Nature*, 2001, **410**, 450–453.

28 (*a*) A. M. Alfantazi and R. R. Moskalyk, *Miner. Eng.*, 2003, **16**, 687–694; (*b*) M. C. B. Fortes and J. S. Benedetto, *Miner. Eng.*, 1998, **11**, 447–451; (*c*) S. Nishihama, T. Hirai and I. Komasawa, *Ind. Eng. Chem. Res.*, 1999, **38**, 1032–1039.

29 F. Hoshyargar, H. Khan, K. Kalantar-zadeh and A. P. O'Mullane, *Chem. Commun.*, 2015, **51**, 14026–14029.

30 (*a*) Z. Li, X. Tao, Y. Cheng, Z. Wu, Z. Zhang and H. Dang, *Mater. Sci. Eng., A*, 2005, **407**, 7–10; (*b*) Y. Zhao, Z. Zhang and H. Dang, *J. Phys. Chem. B*, 2003, **107**, 7574–7576.

31 (*a*) R. G. Alargova, D. S. Warhadpande, V. N. Paunov and O. D. Velev, *Langmuir*, 2004, **20**, 10371–10374; (*b*) B. P. Binks and T. S. Horozov, *Angew. Chem.*, 2005, **117**, 3788–3791; (*c*) U. T. Gonzenbach, A. R. Studart, E. Tervoort and L. J. Gauckler, *Angew. Chem., Int. Ed.*, 2006, **45**, 3526–3530.

32 S. I. Karakashev, O. Ozdemir, M. A. Hampton and A. V. Nguyen, *Colloids Surf., A*, 2011, **382**, 132–138.

33 S. Avivi, Y. Mastai, G. Hodes and A. Gedanken, *J. Am. Chem. Soc.*, 1999, **121**, 4196–4199.

34 (*a*) N. Horasawa, H. Nakajima, S. Takahashi and T. Okabe, *Dent. Mater. J.*, 1997, **16**, 200–208; (*b*) M. R. Khan, C. Trlica and M. D. Dickey, *Adv. Funct. Mater.*, 2015, **25**, 671–678.

35 S. J. French, D. J. Saunders and G. W. Ingle, *J. Phys. Chem.*, 1937, **42**, 265–274.

36 L. Ren, J. Zhuang, G. Casillas, H. Feng, Y. Liu, X. Xu, Y. Liu, J. Chen, Y. Du, L. Jiang and S. X. Dou, *Adv. Funct. Mater.*, 2016, **26**, 8111–8118.

37 (*a*) Y. C. Zhang, X. Wu, X. Y. Hu and Q. F. Shi, *Mater. Lett.*, 2007, **61**, 1497–1499; (*b*) C.-C. Huang and C.-S. Yeh, *New J. Chem.*, 2010, **34**, 103–107; (*c*) Y. Zhao, R. L. Frost and W. N. Martens, *J. Phys. Chem. C*, 2007, **111**, 16290–16299; (*d*) Y. Zhao, R. L. Frost, J. Yang and W. N. Martens, *J. Phys. Chem. C*, 2008, **112**, 3568–3579; (*e*) Y. Quan, D. Fang, X. Zhang, S. Liu and K. Huang, *Mater. Chem. Phys.*, 2010, **121**, 142–146; (*f*) M. Sun, D. Li, W. Zhang, X. Fu, Y. Shao, W. Li, G. Xiao and Y. He, *Nanotechnology*, 2010, **21**, 355601.

38 C.-C. Huang, C.-S. Yeh and C.-J. Ho, *J. Phys. Chem. B*, 2004, **108**, 4940–4945.

39 (*a*) H. Friedman, S. Reich, R. Popovitz-Biro, P. von Huth, I. Halevy, Y. Koltypin, A. Gedanken and Z. Porat, *Ultrason. Sonochem.*, 2013, **20**, 432–444; (*b*) V. B. Kumar, A. Gedanken and Z. Porat, *Ultrason. Sonochem.*, 2015, **26**, 340–344.

40 H.-S. Qian, P. Gunawan, Y.-X. Zhang, G.-F. Lin, J.-W. Zheng and R. Xu, *Cryst. Growth Des.*, 2008, **8**, 1282–1287.